J|A|C|S
ARTICLES
Published on Web 10/23/2004

Probing Molecular Interfaces Using 2D Magic-Angle-Spinning NMR on Protein Mixtures with Different Uniform Labeling

Manuel Etzkorn,[†] Anja Böckmann,*[,‡] Adam Lange,[†] and Marc Baldus*[,†]

Contribution from the Max-Planck-Institute for Biophysical Chemistry, Department of NMR-based Structural Biology, Am Fassberg 11, 37077 Göttingen, Germany, and Institut de Biologie et Chimie des Protéines, UMR 5086 CNRS-UCBL, IFR128 BioSciences Lyon-Gerland, 7, passage du Vercors, 69367 Lyon, France

Received April 11, 2004; E-mail: a.bockmann@ibcp.fr; maba@mpibpc.mpg.de

Abstract: A general NMR strategy to directly study molecular interfaces under magic angle spinning is introduced. The approach is based on the spectroscopic analysis of uniformly, but heterogeneously, labeled molecular mixtures containing the spin species X and Y (X:Y). For the case of an (^{15}N:^{13}C) labeled sample, the use of NC, NHC, and NHHC transfers is demonstrated. Applied to the (^{13}C:^{15}N) labeled dimeric form of the 85 amino acid protein Crh, the NHHC approach reveals a variety of monomer−monomer interactions in the microcrystalline state.

1. Introduction

Intermolecular contacts often provide the microscopic basis for molecular structure and function, ranging from the definition of macroscopic sample properties in material science applications to the control of cellular processes. In the latter case, protein−protein complexes, oligomerization during protein folding, or ligand binding to membranes or membrane receptors exemplify conditions where such interactions can occur in a noncrystalline and insoluble environment. As demonstrated in enzyme−substrate complexes,[1] membrane peptides,[2] and amyloid fibrils,[3] intermolecular contacts can be readily probed by solid-state nuclear magnetic resonance (ssNMR) methods. In these studies, mutagenesis, X-ray/NMR structures, or other biophysical parameters were used to place specific isotope labels in the molecular region of interest. Using ssNMR schemes[4] that permit probing of individual dipolar couplings under magic angle spinning (MAS[5]) conditions, the through-space distance between spin X and Y (Figure 1a) can be subsequently determined. This approach can also be applied if one of the two spin species occurs in high natural abundance but only in a limited number of atomic positions[6] (Figure 1b), but the extension to applications that investigate entire molecular segments in a single experiment is difficult. Such information becomes accessible if multiply or uniformly labeled protein variants are studied. Here, substantial progress in ssNMR methodology has recently led to the near-complete sequential resonance assignments of several microcrystalline proteins.[7,8]

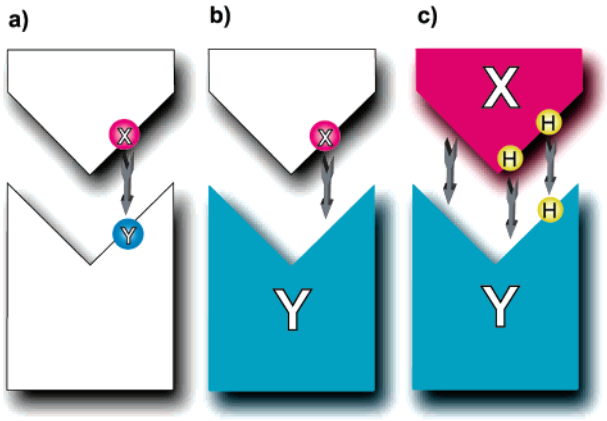

Figure 1. Strategies to investigate molecular interfaces using solid-state NMR. In (a), individual distance constraints are established by applying dipolar recoupling schemes to specifically (X,Y) labeled molecular mixtures. Multiple, or uniform, labeling on one molecular segment permits the probing of nearest neighbor (X:Y) interactions for a particular X nucleus (b). In (c), uniform labeling of both molecular segments permits the study of the entire molecular interface. As discussed in the text, the transfer mechanism can involve (X,Y), (XH,Y), or (XH,HY) spin interactions.

Intermolecular contacts have been detected in multiply labeled samples[9] but require additional information to ensure a reliable

[†] Max-Planck-Institute for Biophysical Chemistry.
[‡] Institut de Biologie et Chimie des Protéines.

(1) Christensen, A. M.; Schaefer, J. *Biochemistry* **1993**, *32*, 2868−2873.
(2) Hirsh, D. J.; Hammer, J.; Maloy, W. L.; Blazyk, J.; Schaefer, J. *Biochemistry* **1996**, *35*, 12733−12741. Fu, R. Q.; Cotten, M.; Cross, T. A. *J. Biomol. NMR* **2000**, *16*, 261−268. Smith, S. O.; Smith, C.; Shekar, S.; Peersen, O.; Ziliox, M.; Aimoto, S. *Biochemistry* **2002**, *41*, 9321−9332.
(3) Benzinger, T. L. S.; Gregory, D. M.; Burkoth, T. S.; Miller-Auer, H.; Lynn, D. G.; Botto, R. E.; Meredith, S. C. *Proc. Natl. Acad. Sci. U.S.A.* **1998**, *95*, 13407−13412. Antzutkin, O. N.; Balbach, J. J.; Leapman, R. D.; Rizzo, N. W.; Reed, J.; Tycko, R. *Proc. Natl. Acad. Sci. U.S.A.* **2000**, *97*, 13045−13050.
(4) McDowell, L. M.; Schaefer, J. *Curr. Opin. Struct. Biol.* **1996**, *6*, 624−629. Griffin, R. G. *Nat. Struct. Biol.* **1998**, *5*, 508−512. Dusold, S.; Sebald, A. *Annu. Rep. NMR Spectrosc.* **2000**, *41*, 185−264.
(5) Andrew, E. R.; Bradbury, A.; Eades, R. G. *Nature* **1958**, *182*, 1659.
(6) Kaustov, L.; Kababya, S.; Du, S. C.; Baasov, T.; Gropper, S.; Shoham, Y.; Schmidt, A. *J. Am. Chem. Soc.* **2000**, *122*, 2649−2650.
(7) Pauli, J.; Baldus, M.; van Rossum, B.; de Groot, H.; Oschkinat, H. *Chembiochem* **2001**, *2*, 272−281. Igumenova, T. I.; Wand, A. J.; McDermott, A. E. *J. Am. Chem. Soc.* **2004**, *126*, 5323−5331. Igumenova, T. I.; McDermott, A. E.; Zilm, K. W.; Martin, R. W.; Paulson, E. K.; Wand, A. J. *J. Am. Chem. Soc.* **2004**, *126*, 6720−6727.
(8) Böckmann, A.; Lange, A.; Galinier, A.; Luca, S.; Giraud, N.; Heise, H.; Juy, M.; Montserret, R.; Penin, F.; Baldus, M. *J. Biomol. NMR* **2003**, *27*, 323−339.

10.1021/ja0479181 CCC: $27.50

distinction between intra- and intermolecular interactions. In the following, we introduce a general NMR strategy to directly study molecular interfaces under MAS conditions. Our approach is based on the spectroscopic analysis of mixtures composed of different molecules, uniformly labeled with spin species X or Y (denoted X:Y, Figure 1c). The evolution and detection periods of a two-dimensional correlation experiment are to be connected by a mixing unit that is only sensitive to the intermolecular region. A direct (X→Y) transfer mechanism must involve through-space dipolar couplings that are actively reintroduced using an appropriate mixing sequence. The effective dipolar coupling hence depends on the internuclear distance and, in particular, on the gyromagnetic ratios γ(X) and γ(Y). Alternatively, polarization may first be transferred to a local proton spin, leading to an enhancement of the dipolar coupling for a given distance, proportional to the ratio $\gamma(^1H)/\gamma(X)$. Finally, homonuclear mixing can be applied if polarization originating from the X species is relayed to nearby ^{1}H spins and subsequently read out after a short (^{1}H,Y) transfer. In the following, we demonstrate these three different transfer mechanisms for the case of (^{13}C:^{15}N) labeled samples. Both types of uniform labeling patterns can be easily obtained in proteins by supplementing isotope labeled starting material such as ^{15}N-labeled NH_4Cl or ^{13}C-labeled glucose, during expression in bacterial cell lines. Moreover, NMR signals in evolution and detection periods can be readily compared to NCA/NCO-type correlation experiments tailored to backbone and side-chain assignments.[7,8,10] We study the efficiency and spinning speed dependence of the different transfer mechanisms for a model system and subsequently demonstrate the use of the concept in the context of the protein Crh, which has been shown to exist in a monomeric form and in a domain swapped dimeric form.[11]

2. Experimental Methods

^{15}N-labeled, ^{13}C (C′,Cα) labeled, and uniformly (^{13}C,^{15}N) labeled versions of glycine were purchased from CIL (Andover, MA). Mixed crystals were obtained by dissolving equal amounts of ^{15}N-labeled and ^{13}C (C′,Cα) labeled Gly in 1 M HCl and subsequent slow solvent evaporation. Uniformly ^{13}C- and ^{15}N-enriched Crh was prepared as described previously.[12] A total of approximately 8 mg of equal amounts of ^{15}N and ^{13}C labeled Crh were mixed under denaturing conditions (8 M guanidinium chloride). The proteins were renatured by 10-fold dilution into 20 mM NH_4HCO_3 buffer and desalted. The mixture was crystallized as described previously[8] by precipitation with 20% PEG 6000 in a crystallization plate over a 2 M NaCl solution. The precipitate was centrifuged directly into a 4 mm CRAMPS rotor, and the rotor cap was sealed. All ssNMR experiments were conducted on wide-bore NMR instruments (Bruker Biospin, Germany) using 4 and 2.5 mm triple resonance (^{1}H,^{13}C,^{15}N) MAS probeheads at 9.4 T (^{1}H resonance frequency 400 MHz) or 14.1 T (^{1}H resonance frequency 600 MHz) at a temperature of −5 °C. NC cross polarization (CP) transfer was established using conventional Hartmann−Hahn[13] matching conditions employing radio frequency (rf) fields comparable to the isotropic chemical shift difference (δC′−δCα) and by placing the carrier frequency close to on-resonance for each target spin.[14] In this way, on-resonance ^{1}H decoupling can be used during mixing, and additional off-resonance proton−proton decoupling schemes[15] to prevent CP leakage during NC contact are not necessary. TPPM proton decoupling[16] was applied during evolution and detection periods.

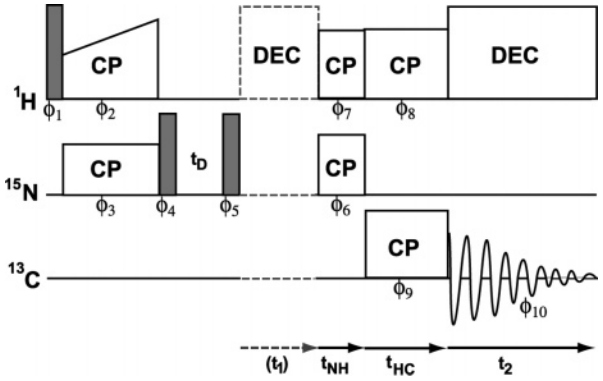

Figure 2. Pulse scheme for one- or two-dimensional NHC polarization transfer under MAS conditions. The complete phase cycle is given as Supporting Information.

In Figure 2, the pulse scheme for one- or two-dimensional NHC polarization transfer is shown. After an initial CP transfer and a z filter to remove any residual ^{1}H magnetization, ^{15}N chemical shifts are recorded along the (optional) t_1 evolution time. Next, a short CP step ensures that only ^{1}H magnetization of $N(H)_x$ groups is created. Establishing (^{1}H,^{13}C) CP for a variable mixing time t_{HC} allows for transfer to nearby ^{13}C spins that is read out along t_2. Note that the pulse scheme described[17] can be modified to include a homonuclear (^{1}H,^{1}H) decoupling unit during (^{1}H,^{13}C) CP. The 1D NHC experiments discussed below were performed by setting t_1 to zero and incrementing t_{HC}. NHHC transfer was established using the pulse scheme given in refs 18 and 19. NH and HC transfer steps bracketing the (^{1}H↔^{1}H) mixing unit were set to 200 and 80 μs, respectively.

All numerical simulations were conducted using the NMR simulation environment GAMMA.[20] NC transfer was computed assuming an isolated two-spin system under rf fields during CP and MAS rates, as given by the experimental setup. The spin dynamics under NHC transfer conditions were simulated assuming a 7-spin system consisting of three ^{1}H spins of the NH_3 group, a C′ spin, and a $C_\alpha H_2$ group. As in the NC case, the transfer dynamics were monitored assuming a piece-wise constant system Hamiltonian.[10] Finally, the experimental transfer characteristics of the NHHC experiments under longitudinal mixing were analyzed using the relaxation model of ref 19. Here, polarization transfer within a dipolar coupled proton bath is described by a zero-quantum relaxation rate that depends on the internuclear distance between the two proton spins of interest and the MAS rate.

3. Results and Discussion

First, we conducted a series of polarization transfer experiments on isotope labeled versions of a simple amino acid for which structural information relating inter and intramolecular contacts is available. In Figure 3, experimental results obtained on a uniformly (^{13}C,^{15}N) labeled sample and on a (^{13}C:^{15}N)

(9) Tycko, R.; Ishii, Y. *J. Am. Chem. Soc.* **2003**, *125*, 6606−6607. de Boer, I.; Matysik, J.; Amakawa, M.; Yagai, S.; Tamiaki, H.; Holzwarth, A. R.; de Groot, H. J. M. *J. Am. Chem. Soc.* **2003**, *125*, 13374−13375.
(10) Baldus, M. *Prog. Nucl. Magn. Reson. Spectrosc.* **2002**, *41*, 1−47.
(11) Juy, M.; Penin, F.; Favier, A.; Galinier, A.; Montserret, R.; Haser, R.; Deutscher, J.; Böckmann, A. *J. Mol. Biol.* **2003**, *332*, 767−776.
(12) Penin, F.; Favier, A.; Montserret, R.; Brutscher, B.; Deutscher, J.; Marion, D.; Galinier, A. *J. Mol. Microbiol. Biotechnol.* **2001**, *3*, 429−432.
(13) Hartmann, S. R.; Hahn, E. L. *Phys. Rev.* **1962**, *128*, 2042−2053.
(14) Baldus, M.; Petkova, A. T.; Herzfeld, J.; Griffin, R. G. *Mol. Phys.* **1998**, *95*, 1197−1207.
(15) Baldus, M.; Geurts, D. G.; Hediger, S.; Meier, B. H. *J. Magn. Reson., Ser. A* **1996**, *118*, 140−144.
(16) Bennett, A. E.; Rienstra, C. M.; Auger, M.; Lakshmi, K. V.; Griffin, R. G. *J. Chem. Phys.* **1995**, *103*, 6951−6958.
(17) Lange, A. Diploma thesis, University Goettingen, 2002.
(18) Lange, A.; Luca, S.; Baldus, M. *J. Am. Chem. Soc.* **2002**, *124*, 9704−9705.
(19) Lange, A.; Seidel, K.; Verdier, L.; Luca, S.; Baldus, M. *J. Am. Chem. Soc.* **2003**, *125*, 12640−12648.
(20) Smith, S. A.; Levante, T. O.; Meier, B. H.; Ernst, R. R. *J. Magn. Reson., Ser. A* **1994**, *106*, 75−105. Baldus, M.; Levante, T. O.; Meier, B. H. *Z. Naturforsch., A: Phys. Sci.* **1994**, *49*, 80−88.

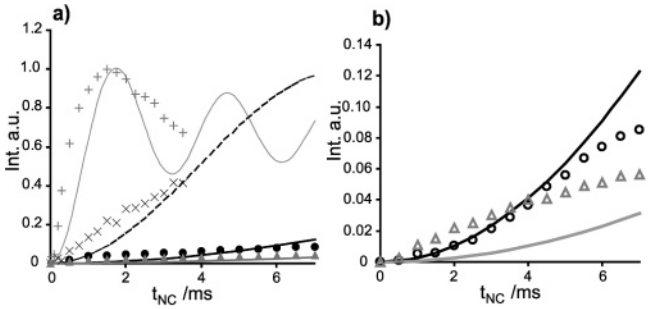

Figure 3. Comparison of experimental N→C polarization transfer dynamics obtained on Gly·HCl (symbols) to quantum-mechanical two-spin simulations (lines). In (a), results of a (^{13}C:^{15}N) labeled variant of Gly·HCl (filled circles/black line, C′; and triangles/thick gray line, Cα) are compared to data obtained on uniformly labeled Gly·HCl (+ symbols/thin gray line, Cα; and X symbols/dashed line, C′) at an MAS rate of 11 kHz. In (b), experimental results for (^{13}C:^{15}N) labeled Gly·HCl are compared to numerical predictions at 25 kHz MAS. Results are shown for N→C′ (circles, black line) and N→Cα (triangles, gray line) transfer. While rf fields of 14 kHz (^{13}C) and 25 kHz (^{15}N) were used during NC transfer at 11 kHz MAS, 6 kHz (^{13}C) and 31 kHz (^{15}N) were employed at 25 kHz.

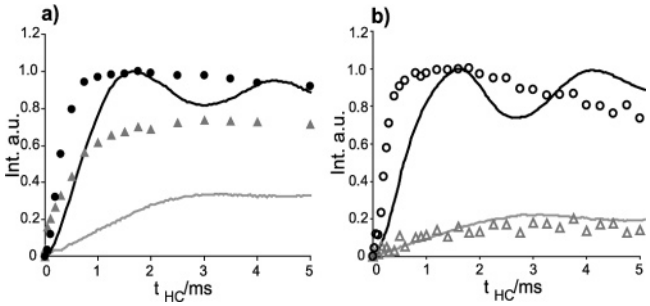

Figure 4. Comparison between experimental (symbols) and theoretical results (black line C′, gray line Cα) of an NHC experiment. The buildup characteristics for C′ (circles) and Cα (triangles) resonances were recorded for an MAS rate of 11 kHz (a) and 25 kHz (b). Numerical results (lines) were obtained assuming a 7-spin system. A z filter time t_D of 3 ms was used. Rf fields during HC transfer were set to 39 kHz (^{13}C) and 50 kHz (^{1}H) in (a) and 39 kHz (^{13}C) and 64 kHz (^{1}H) in (b).

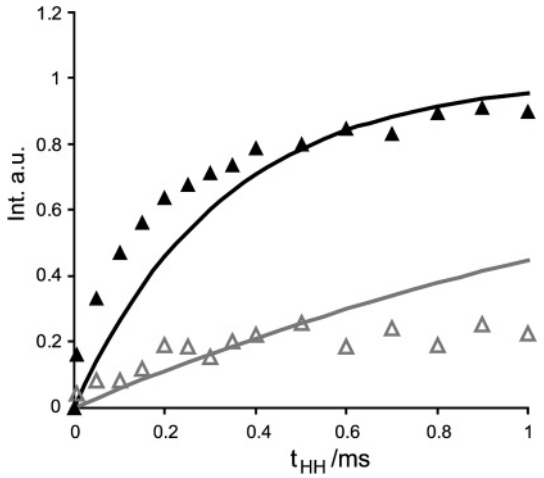

Figure 5. NHHC transfer for 11 kHz (▲) and 25 kHz (△) on (^{13}C:^{15}N) labeled Gly·HCl. Theoretical results were obtained by calculation of an exponential signal buildup using an (NH−HCα) distance of 3.2 Å and the zero-quantum line-shape functions given in ref 19 for 11 kHz (black line) and 25 kHz (gray line).

labeled variant of Gly·HCl are compared to quantum-mechanical (QM) two-spin simulations for an MAS rate of 11 kHz (a) and 25 kHz (b). For the uniformly labeled sample, the transfer dynamics follow the QM predictions assuming an N−C distance of 1.46 Å (N,Cα) and 2.43 Å (N,C′) expected from intramolecular polarization transfer. Better agreement between theory and experiments may be obtained by including rf inhomogeneity effects. A comparison of the observed buildup characteristics for the (^{13}C:^{15}N) labeled sample (indicated by triangles and circles) with intermolecular distances found in the crystal structure[21] reveals that the results of the N→C transfer experiment are in qualitative agreement with the X-ray structure for both MAS rates. The shortest intermolecular distances are given by 3.84 and 4.85 Å for N→C′ (circles) and N→Cα (triangles) transfer, respectively. Due to the low gyromagnetic ratio, NC transfer hence requires relatively long mixing times for a given intermolecular ^{15}N−^{13}C distance, and the data in Figure 3 only reflect the initial rate regime dependence. Notably, the experimental and theoretical results are largely independent of the MAS rate, as expected for polarization transfer under the CP dipolar recoupling sequence.

Similar to Figure 3, NHC data shown in Figure 4 for the C′ and Cα spin pair were recorded for an MAS rate of 11 kHz (a) and 25 kHz (b). According to the crystal structure, the shortest intermolecular distances are given by 3.04 and 4.12 Å for the (NH,C′) and (NH,Cα) pair, respectively. As revealed by the numerical simulations conducted for a 7-spin (H_3−C′−CαH_2) system, the transfer dynamics should be rather unaffected by the change of the MAS rate (11 kHz, Figure 4a vs 25 kHz, Figure 4b). Indeed, the experimental NH→C′ transfer profile largely agrees with the QM simulations, revealing a local maximum at 2 ms. Differences between experiment and simulation may result from resonance offsets that in general lead to a faster oscillation (data not shown), rf inhomogeneity effects, as well as multiple-spin interactions not included in the simulations. Such effects, however, fail to account for the large differences in NH−Cα transfer efficiency that is strongly dependent on the MAS rate and only agrees with the QM simulation at 25 kHz. Notably, these deviations are not removed by applying homonuclear (^{1}H,^{1}H) decoupling schemes such as Lee−Goldburg irradiation[22] during Hartmann−Hahn transfer because the dominating effects are related to strong (^{13}C,^{1}H) interactions that are not suppressed by homonuclear decoupling sequences. As described in further detail in ref 10, the decreased efficiency for the NH→Cα transfer can be well explained by polarization leakage to the neighboring proton spins that limit the buildup of Cα magnetization during NHC contact. Interestingly, these interactions seem to be of less relevance for an MAS rate of 11 kHz. We attribute these deviations to multiple-spin effects that broaden the HH transfer profile and here render NHC polarization transfer more efficient.

Finally, Figure 5 demonstrates the use of the NHHC transfer profile for a (^{13}C:^{15}N) labeled sample of glycine at two different MAS rates. In both cases, experimental buildup rates are compared to theoretical predictions using the relaxation-based analysis of ref 19 and intermolecular NH−HCα distances of 3.2 Å. For both MAS rates, theory and experimental results are in good agreement. The efficiency of the transfer methods under investigation is depicted in Figure 6 at an MAS rate of 11 kHz.

(21) Alkaraghouli, A. R.; Cole, F. E.; Lehmann, M. S.; Miskell, C. F.; Verbist, J. J.; Koetzle, T. F. *J. Chem. Phys.* **1975**, *63*, 1360−1366.

(22) Lee, M.; Goldburg, W. I. *Phys. Rev.* **1965**, *140*, 1261−1271.

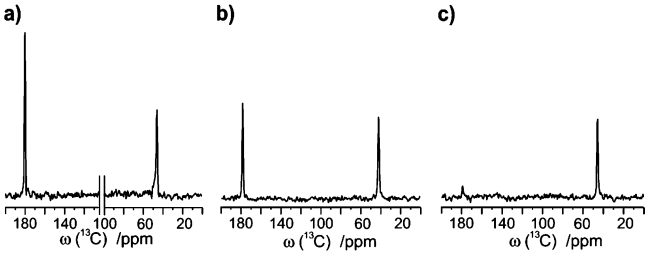

Figure 6. 1D slices with maximal (for the mixing times considered in Figures 3−5) signal intensity obtained on (^{13}C:^{15}N) labeled Gly·HCl for (a) NC (256 scans), (b) NHC (128 scans), and (c) NHHC (192 scans) transfer. In (a), results of two separate experiments (i.e., N→C′ and N→Cα, separated by vertical lines) are shown that were obtained using a ^{13}C carrier frequency close to the carbon resonance of interest.

For the range of mixing times considered, NC, NHC, and NHHC are described by comparable transfer efficiencies, which amount to 5−10% of the directly detected ^{13}C CP signal.

Because spin pairs exhibiting the largest gyromagnetic ratio are probed, the NHHC experiment is particularly attractive to study interface regions of variable volume. The NHHC approach was hence applied to a microcrystalline sample of the protein Crh for which we have recently reported ssNMR resonance assignments.[8] Analysis of the conformation-dependent chemical shifts suggested that the protein forms, similar to the single-crystal structure,[11] a domain-swapped dimer in the microcrystalline state. Each chain hence not only consists of the βαββαβα motif previously observed for the monomeric form,[23] but includes an additional short β-strand, referred to as β1a. The electron density map unambiguously revealed a domain swap at the dimer interface. Thus, the β1a-strands of each chain connect to build an interchain antiparallel β-sheet in the hinge region. Consequently, the β1-strand of one chain forms hydrogen bonds to the β4-strand of the other in an antiparallel manner, thereby completing the 4-strand β-sheet. This β1-strand swapping results in a tight dimer association due to an extensive dimer interface, with numerous main-chain and side-chain contacts observed between the two polypeptide monomers. Table 1 (see Supporting Information) contains all contacts up to 4 Å and a selected set of interactions in the 4−4.5 Å range (vide infra) between nitrogen-bound and carbon-bound protons in the Crh dimer crystal structure (PDB entry 1mu4, ref 11). These constraints were classified into intra-dimer and inter-dimer contacts comprising backbone NH or side-chain nitrogen-bound protons. The observed interactions mainly relate to protein segments directly concerned by the β-1 strand domain swap, residues Met1−Gln15, including β-strands 1 (residues Val2−Glu7) and 1a (residues Thr12−Leu14), as well as β-strand 4 (residues Glu60−Gln66). Residues Ser56−Thr59 from loop 2 (residues Leu53−Thr59) near the hinge region exhibit several contacts. Some interactions concern, in addition, helices A (residues Ala16−Asn27) and C (residues Glu70−Gln82). Glutamine side chains are heavily involved in intra- as well as inter-dimer contacts: 6 out of the 8 Gln show a total of 25 contacts, many of them for protons closer than 3 Å. In the Crh single crystal, the dimer packs loosely in the crystals (with a high water content of about 70%), and only a small number of inter-dimer contacts involving backbone amide protons are found (see Table 1, Supporting Information).

(23) Favier, A.; Brutscher, B.; Blackledge, M.; Galinier, A.; Deutscher, J.; Penin, F.; Marion, D. *J. Mol. Biol.* **2002**, *317*, 131−144.

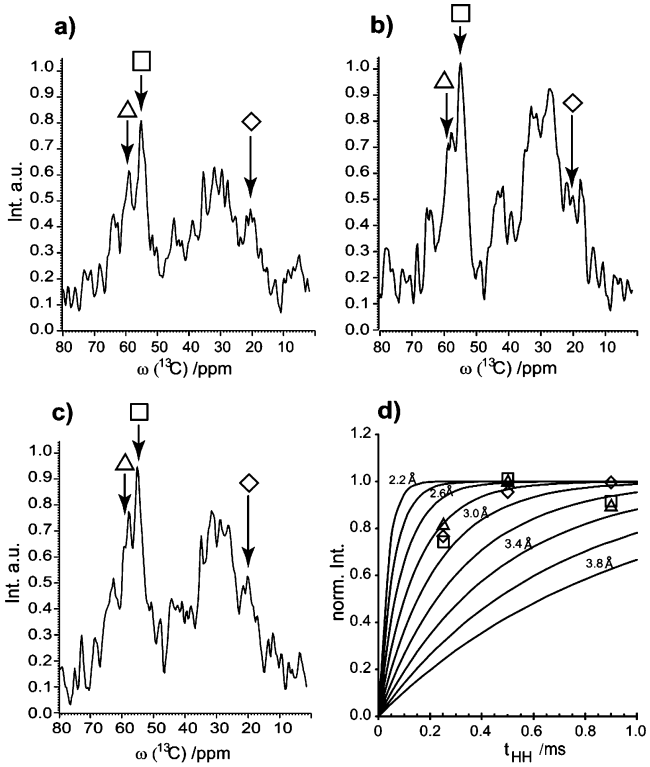

Figure 7. (a−c) 1D NHHC spectra (14k scans) with proton mixing times of 250, 500, and 900 μs, respectively. (d) Comparison of the (normalized) signal intensities for selected ^{13}C resonance frequencies to theoretical buildup curves deduced from ref 19. Symbols reflect NMR signal intensities measured at the following ^{13}C resonance frequencies: $\omega(^{13}C) = 59.1$ ppm (△, equivalent to Cα shift of Thr12) and $\omega(^{13}C) = 19.8$ ppm (◇, equivalent to Cα shift of Val6). As in the case of $\omega(^{13}C) = 55$ ppm (□), the observed signal intensity may, however, result from more than one protein residue.

To directly probe intermolecular contacts in the microcrystalline state, we first conducted a series of 1D NHHC experiments on (^{13}C:^{15}N) labeled Crh for increasing proton−proton mixing times (Figure 7a−c). These spectra can be used to investigate the relationship between the theoretical transfer buildup rate[19] (Figure 7d) and the observed signal intensity for distinct side-chain resonance frequencies. Due to incomplete ^{13}C spectral resolution, such a study does not allow for an analysis of individual (NH→HC) transfers. However, the overall buildup characteristics observed experimentally are in qualitative agreement with intramolecular NHHC studies,[19] where a proton−proton mixing time (t_{HH}) of 500 μs leads to the detection of (^{1}H,^{1}H) intermolecular transfers of about 3.5 Å. The corresponding 2D spectrum (Figure 8) reveals a variety of backbone−backbone and backbone−side-chain contacts. They were analyzed using solid-state NMR resonance assignments reported previously.[8] Due to the lower spectral resolution and sensitivity, increased error margins were assumed as compared to the case of U-[^{13}C,^{15}N] labeled Crh. Distance information was obtained from the X-ray diffraction data[11] (see Table 1, Supporting Information). For the selected mixing time and in view of the results of the 1D buildup experiments, most of the observed correlations must be mediated by two-spin (^{1}H,^{1}H) interactions. While no inter-dimer contacts could be detected, a total of 19 residues found at the dimer interface yield monomer−monomer cross signals corresponding to internuclear distances below 4 Å. Five additional correlations can be explained by intermonomer contacts in the range of 4−4.5 Å.

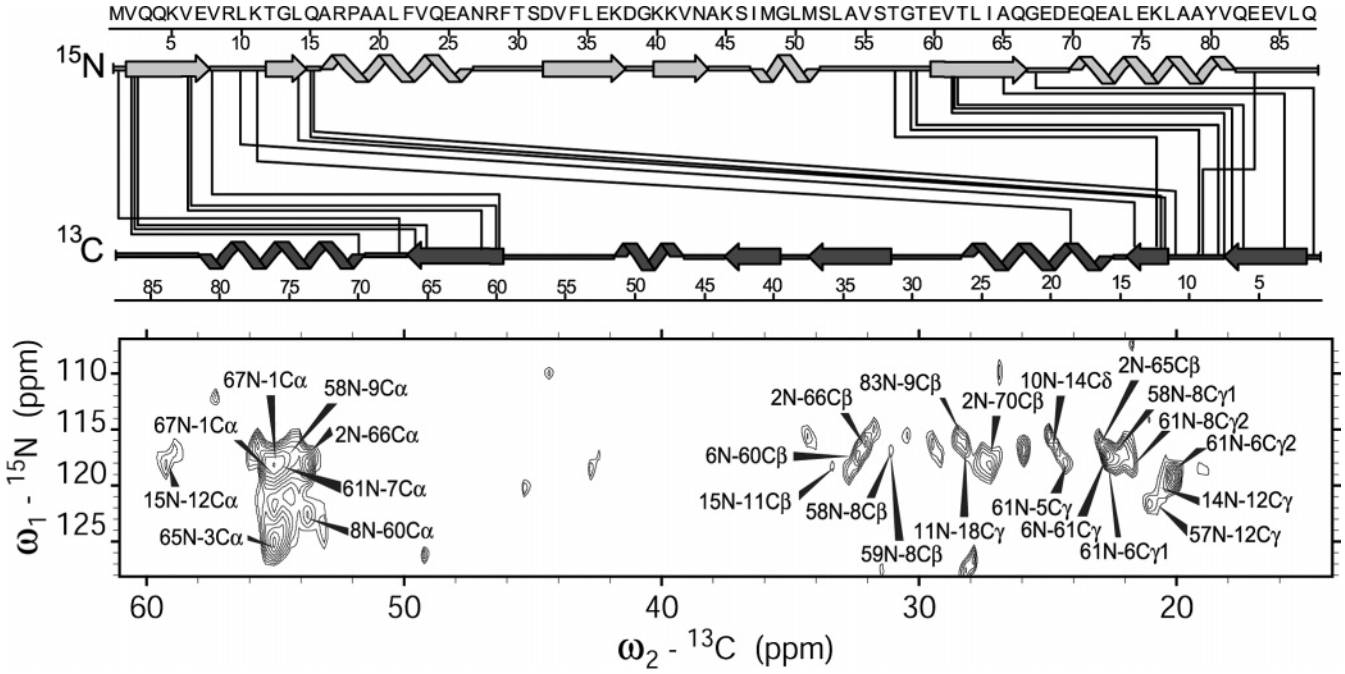

Figure 8. Results of an NHHC[18,19] experiment conducted on a (^{13}C:^{15}N) labeled microcrystalline sample of Crh. The spectrum was recorded at 600 MHz using an MAS rate of 11 kHz and $T = -8$ °C. Longitudinal proton−proton mixing (t_{HH}) was allowed for 500 μs. Results of several 2D experiments (total 28k scans per t_1 experiment, 14 t_1 experiments) were added. The spectrum was processed using a Lorentzian line broadening of 50 Hz and was further analyzed using Sparky version 3.106 (T. D. Goddard and D. G. Kneller, University of California, San Francisco). Monomer−monomer contacts consistent with the reported Crh dimer structure are indicated in the spectrum (bottom) and the amino acid sequence (top).

These correlations are indicated along the polypeptide chains in Figure 8. Val2 and Val6 show transfers to their respective hydrogen-bonding partners in the antiparallel β-sheet Ala65 and Val61, as well as to the neighboring Gln66 and Glu60. Gln3 exhibits magnetization exchange with Ala65 NH, and Lys5 and Glu7 from Val61 NH. Val8 reveals multiple transfers from or to Gly58, Thr59, Glu60, and Val61. Arg9 shows a cross signal with Gly58. In the hinge region, several pairs reflect the close connection between the two monomers: Leu10−Leu14, Lys11−Gln15, and Thr12−Leu14, Gln15. In addition to contacts involving Gly58 and Thr59, interactions between Thr57 and Thr12 reveal the partaking of loop 2 in the dimer interface, close to the hinge region. Val2/Glu70 and Lys11/Pro18 are the only contacts involving helices A and C.

Cross-peak correlations observed in Figure 8 at 117.1/119.5 (^{15}N) and 55 ppm (^{13}C) are consistent with interactions between Gly67 NH (Gly67 NH exhibits doubled ^{15}N resonance signals[8]) and Met1 Cα. They not only confirm our recent assignment of Met1 Cα,[24] but also indicate that protein mobility does not prohibit intermolecular polarization transfer at the N-terminus. In contrast and in line with weak cross-peak signals in intramolecular Crh correlation spectra,[8] many correlations involving Val81, Glu82, and Glu83 are not observed, indicative of increased mobility of the C-terminal residues.

Because NHHC mixing is mediated by the combined effect of two dipolar, one-bond (^{15}N→^{1}H, ^{1}H→^{13}C) interactions, and one relaxation-mediated (^{1}H→^{1}H) through-space transfer, NMR signals originating from regions of increased molecular mobility will be attenuated. Hence, cross-peak signals expected for methyl groups and NH_3^+ nitrogen spins are in general weak or missing. Unlike Arg and Lys side chains, NMR resonances of glutamine Nϵ2 and asparagine Nδ2 groups are expected in the considered ^{15}N spectral window. However, the corresponding correlations are not detected in Figure 8, probably due to increased mobility.

The absence of correlations concerning Gln4 may be due to the hydrophilic character of the Q3−K5 stretch, leading to side chains oriented toward the solvent environment. Such interactions seem to be less stabilizing than the strong hydrophobic interactions observed, for example, for Val2 and Val6, which form part of the hydrophobic core. Interestingly, no correlations could be observed for Leu63 that represents the hydrogen-bonding partner of Gln4 in the β-sheet formed by β-strands 1 and 4. These experimental observations could point to differences in the dynamical behavior along the polypeptide chain. In summary, many monomer−monomer contacts expected from the single crystal study but not detected in the 2D ssNMR experiment on a microcrystalline sample can be related to regions of increased molecular mobility. Figure 9 visualizes the monomer−monomer contacts observed in the NMR experiments and predicted from the 3D Crh crystal structure.

In protein−protein complexes of the size considered or larger, 2D spectroscopy will in general not be sufficient to unambiguously assign all (^{15}N,^{13}C) resonances in the ssNMR spectrum. To obtain unequivocal spectral assignments, 3D spectroscopy that, for example, incorporates intramolecular (^{13}C,^{13}C) correlations will be beneficial. In other studies, chemical-shift information will only be available for one molecule. In this case, the spectrally unassigned, possibly larger protein may solely serve as a source of polarization that is transferred to the known fragment and can subsequently be analyzed using multidimensional correlation spectroscopy on the target protein only. As shown here, (^{13}C:^{15}N) labeling represents an attractive approach for applications in polypeptides. While protein−protein interactions may also be studied using ^{13}C block-labeled[25] or partially deuterated (^{1}H:^{2}H,^{13}C) mixtures, novel insight into the details

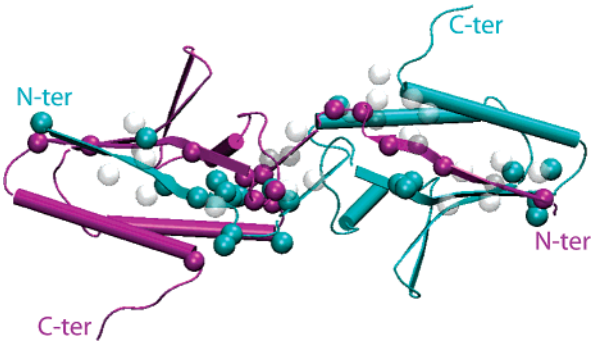

Figure 9. Intermonomer contacts reported on the Crh 3D crystal structure (PDB entry 1mu4). Contacts observed in the NHHC correlation spectrum are shown in purple for the NH nitrogen, and in blue for the different carbon atoms. Contacts between nitrogen atoms (dark gray) and carbon atoms (light gray) predicted from the single-crystal structure and not observed in the 2D NHHC spectrum are included.

of protein−DNA or protein−membrane interactions may result from (^{13}C,^{15}N:^{31}P) 2D ssNMR spectroscopy.

4. Conclusions

All considered NMR schemes are capable of probing intermolecular interactions under MAS conditions. Application of the NHHC concept maximizes spectral resolution and the detectable distance between the two proteins of interest. Unlike the NC approach, the NHHC scheme does not necessitate careful optimization of CP transfer steps involving weak (intermolecular) dipolar interactions. Because NC and NHC transfers are based on a nonvanishing dipolar coupling element, they may be favorable in the case of applications under ultrafast MAS where relaxation-mediated transfer is attenuated[19] or for the investigation of nonprotonated target spins. For all considered ssNMR schemes, no advanced sample preparation methods are necessary, and a multitude of structural constraints can be obtained from a single 2D experiment. For the Crh dimer where spectral assignments are on hand for both monomer units, numerous intermolecular contacts could be observed in the spectrum and assigned to residues at the dimer interface. Differences in the correlation pattern expected from the single-crystal structure might point to regions of increased molecular mobility. Hence, the combination of X-ray and the solid-state NMR approach outlined here may provide a sensitive tool to monitor protein dynamics at molecular interfaces.

If resonance frequencies for one or even both molecular interface units are not available, standard chemical shift information could be combined with other structural or biophysical parameters (e.g., resulting from mutagenesis experiments) to test or refine structural models of the binding interface. Such attempts could involve protein−protein docking or homology modeling routines.[26] Analogous approaches may also be useful in characterizing interactions between modular proteins.[27] Finally, comparison of the signal-to-noise ratio between a reference compound and the application of interest could be used to estimate the probability of finding intermolecular contacts in the NMR sample under study, which, for example, is relevant in the context of understanding oligomerization processes during protein aggregation or in the case of multisite binding events in (membrane) proteins.

Acknowledgment. This work was funded in part by CNRS (PICS n°2424), the french research ministry (ACI Biologie Cellulaire Moléculaire et Structurale 2003), and the MPG. A.L. thanks the Stiftung Stipendien Fonds des Verbandes der Chemischen Industrie for a Ph.D. fellowship. Scientific discussions with Dr. C. E. Hughes and Dr. H. Heise are gratefully acknowledged.

Supporting Information Available: The detailed phase cycle for the NMR pulse scheme shown in Figure 2 and a table summarizing monomer−monomer contacts in Crh. This material is available free of charge via the Internet at http://pubs.acs.org.

JA0479181

(24) Lesage, A.; Böckmann, A. *J. Am. Chem. Soc.* **2003**, *125*, 13336−13337.
(25) LeMaster, D. M.; Kushlan, D. M. *J. Am. Chem. Soc.* **1996**, *118*, 9255−9264.
(26) Russell, R. B.; Alber, F.; Aloy, P.; Davis, F. P.; Korkin, D.; Pichaud, M.; Topf, M.; Sali, A. *Curr. Opin. Struct. Biol.* **2004**, *14*, 313−324.
(27) Pickford, A. R.; Campbell, I. D. *Chem. Rev.* **2004**, *104*, 3557−3565.